

# Measurement of the permeability tensor in nanophases of granular metal oxides and field-induced magnetic anisotropy

Stéphane Mallégo, Christian Brosseau,\* Patrick Quéffelec, and Anne-Marie Konn

Laboratoire d'Electronique et Systèmes de Télécommunications, Université de Bretagne Occidentale, 6 avenue Le Gorgeu, B.P. 809, 29285 Brest Cedex, France

(Received 23 October 2002; revised manuscript received 27 May 2003; published 19 November 2003)

We have investigated the composition and frequency dependence of the permeability tensor in heterostructures composed of metal oxides nanoparticulate powders. Samples consist of grains of the magnetic phase ( $\gamma$ -Fe<sub>2</sub>O<sub>3</sub>) homogeneously dispersed in a nonmagnetic insulating background (ZnO). A measurement capability has been used to investigate the permeability tensor components of the ferrimagnetic samples under an external magnetic field, as a function of composition. The samples exhibit a previously unobserved field-dependent anisotropic contribution to the permeability tensor. The gyromagnetic resonance frequency decreases with Fe<sub>2</sub>O<sub>3</sub> content and increases with applied magnetic field. The frequency-dependent response in the microwave frequency range can be fit reasonably well using a single parameter whose value is consistent with the determination from a ferromagnetic resonance experiment and can be rationalized by means of a recently developed coarse-grained multiscale model. The model is based on multiscale averaging techniques and takes into account magnetostatic intergranular interactions via a mean-field approximation. These observations are aimed at developing a more realistic description of magnetic nanophases that takes into account details of the microstructure and provide salient input to micromagnetic simulations.

DOI: 10.1103/PhysRevB.68.174422

PACS number(s): 76.50.+g, 66.90.+r, 68.65.-k

## I. INTRODUCTION

Current research indicates that the electromagnetism of nanostructures is a challenging field for experimentalists as well as for theoreticians. Understanding the complexities of electronic and magnetic properties at low dimensions constitutes one of the central focuses of condensed matter physics. During the last decade an enormous amount of effort has gone into studying the effects of size and shape of nanophases and nanometer-scale structures on permittivity and permeability. Along with generic features reported for these compounds such as the fact that the electromagnetic properties of nanostructures often deviate significantly from those of their coarser-grained counterparts, some display exotic properties as well.<sup>1,2</sup> The changes in the electromagnetic properties due to reduction in grain sizes are due to the fact that a high fraction of the overall material is in the vicinity of an interface and to the confinement of electrons and excitons in small volumes. In addition, the properties will be affected by the presence of defects such as impurities and grain boundaries that result from synthesis and processing. From an engineering perspective the source of this abundant interest lies in the potentially very large area of applications ranging from sensors to high-density magnetic recording and microwave circuits.<sup>3</sup> Advances in the compositional development and processing science of granular nanophases suggest them to be promising candidates for costly effective, magnetically tunable microwave device applications such as circulators and isolators, compatible with integrated-circuit and solid-state technology. More specifically, the study of nonreciprocal components which are made possible by selecting the appropriate gyrotropic materials has been the subject of extensive experimental and theoretical work in recent years. From a fundamental standpoint, it is a challenge to

study the propagation of electromagnetic waves in nanostructures using *ab initio* methods, such as the density-functional theory. Although computation simulations of the underlying physics have generated a substantial amount of work over the years (see, e.g., Refs. 4 and 5, and references therein), the experimental work is only recent, and to date only a limited number of measurements have focused on this problem.<sup>6,7</sup> The important questions about the electromagnetism at these length scales can best be resolved by direct experimental observation in real space and eventually yield results against which to benchmark numerical models.

An essential step regarding the development of magnetic nanostructures is the detailed understanding of the nature and source of magnetic anisotropy. However, despite its crucial role, there has been little work dealing explicitly with the permeability of anisotropic and spatially inhomogeneous magnetic materials and its calculation from first principles is a long-standing problem. Attempts to do this have been developed including theoretical approximations assuming in most cases a quasistatic hypothesis without time rescaling<sup>2,4</sup> and numerical methods using a variety of techniques, such as Monte Carlo simulations, a finite-element scheme, or algebraic formulations.<sup>4,5</sup> Early pioneering work by Polder<sup>8</sup> yielded an expression for the permeability of a uniformly magnetized single-domain anisotropic magnetic particle which is described by a second-rank Hermitian tensor

$$\vec{\mu} = \begin{bmatrix} \mu & j\kappa & 0 \\ -j\kappa & \mu & 0 \\ 0 & 0 & 1 \end{bmatrix}$$

in the coordinate system such that the external field is applied in the positive  $z$  direction, where  $\mu = \mu' - j\mu''$  is the effective permeability and  $\kappa = \kappa' - j\kappa''$  is the effective non-

diagonal term, where single prime and double prime denote, respectively, real and imaginary parts. Here the magnetization vector is  $\vec{M} = M_s \vec{z}$ , where  $\vec{z}$  is the unit vector in the equilibrium direction. To complicate the situation further, several authors have considered the case of partially magnetized materials.<sup>9–12</sup> Moreover, a comprehensive multilength-scale description of submicron magnetic particles which can provide detailed information concerning structure and collective magnetic behavior has not been achieved yet and is still a subject of profound discussions in the recent literature.<sup>13,14</sup> The dynamics of magnetization reversal and coercive field in magnetic materials is governed by several interacting processes taking place simultaneously at different length scales. The complexity may be structural in origin, or it may be rooted in the magnetic and electronic interactions having various origins and different energy scales, e.g., spin-exchange interactions and dipole-dipole interactions. For dynamic simulations, the relevant length scales should be coupled. Despite its obvious relevance to our fundamental understanding of magnetism, experimental progress on magnetic anisotropy in nanostructures is constrained by the limitations of available diagnostic techniques.

Over the past decade or so, metal oxides nanopowders have been recognized as model systems for investigating nanostructures.<sup>15</sup> Dense packings of particles are frequently used in these investigations not only because they are economical but also because they are easily processable and allow for unique control over composition and architecture on the nanoscale. Observe that the wide variety of behavior is further complicated by interparticle interactions arising from the difficulty of controlling particle dispersal. In a set of early experiments,<sup>16</sup> we showed that the overall features of the zero-field (isotropic) electromagnetic properties of diluted magnetic ( $\gamma$ - $\text{Fe}_2\text{O}_3$ )-semiconductor (ZnO) granular heterostructures exhibit a strong dependence on the powder size of the starting materials. Furthermore, the analysis of the hysteresis response indicates that the coercivity and the saturation magnetization normalized to the content of  $\text{Fe}_2\text{O}_3$  in the sample remain nearly constant over the entire  $\text{Fe}_2\text{O}_3$  volume fraction range investigated.<sup>16</sup> Over the last few years, we have developed an effective technique<sup>6</sup> with which to achieve accurately measuring both the diagonal and nondiagonal components of the permeability tensor. This technique offers many superior features over other methods for (isotropic) electromagnetic characterization of particulate materials and deserves further exploration.

With the above as motivation, we report in this article on the field and composition dependences of the (anisotropic) electromagnetic transport properties of ZnO and  $\gamma$ - $\text{Fe}_2\text{O}_3$  granular nanostructures. The key objectives of this work are (i) to present the results of our first systematic study of the anisotropic component of the permeability of multicomponent magnetic nanostructures and (ii) to support the implications of our previously mentioned work.<sup>14</sup>

This paper is organized as follows. In Sec. II we describe the experimental details. In Secs. III and IV, we present the results of an investigation of the gyromagnetic resonance mode at different compositions and magnetic fields, and we show that the permeability data can be rationalized within a

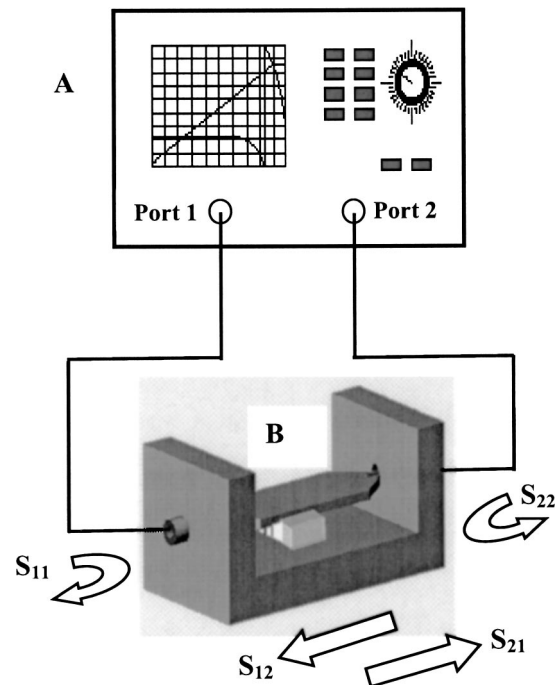


FIG. 1. Schematic diagram of the experimental setup used for permeability tensor measurement. The corresponding experiments have been performed using an HP 8720A network analyzer and a full two-port  $S$  parameter test set (A). Cell and sample geometry (B). We use the notation  $S_{ij}$ ,  $i, j = 1, 2$ , to represent the reflection and transmission scattering parameters from port 1 (2) to port 2 (1).

recently developed approach based on a multilength-scale description of the problem, respectively. Finally, the paper concludes with a summary in Sec. V.

## II. EXPERIMENT

### A. Electromagnetic measurements

In the present work we use a recently developed noniterative experimental characterization method to determine the permeability tensor of magnetic nanocomposites.<sup>6</sup> At the heart of the experiment, our approach involves (see Fig. 1) a nonreciprocal strip transmission line measurement cell which has been partially filled with a  $5 \times 5 \times 1.8 \text{ mm}^3$  rectangular nanocomposite sample. The cell is connected to an HP 8720A automatic network analyzer allowing us to measure the scattering parameters ( $S$  parameters<sup>17</sup>) which represent the reflection and transmission coefficients from port 1 (2) to port 2 (1) of the network analyzer. To accurately obtain its electromagnetic characteristics, the test sample is placed in the space between the conducting strip and lower ground plane of the cell. The microwave energy, indeed, is chiefly located in this region of the cell. The main advantage of employing a nonreciprocal cell is that it allows one to measure separately the  $S$  parameters in order to derive both  $\mu$  and  $\kappa$  in the operating frequency range by a single experiment. To ensure nonreciprocity, the transverse field displacement effects in the propagation structure are exploited.<sup>18</sup> Two steps are necessary. In the first step, a  $5 \times 5 \times 1.8 \text{ mm}^3$  rectangular piece of dense  $\text{TiO}_2$  (rutile) of relative permittivity

$\varepsilon_d = 15.5$  is placed on one side of the test sample, whereas, on the other side, air ensures that the cell cross section is asymmetrically defined. In the second step, the cell is placed between the pole faces of an electromagnet to transversely and uniformly magnetize the sample to be characterized.

The effective permeability tensor components  $\mu$  and  $\kappa$  of the magnetic sample can be presented as<sup>6</sup>

$$\mu(\omega) = \frac{2a\gamma^+\gamma^-}{\mu_0\varepsilon_0\omega^2[(b-a)(1+\varepsilon_d)+2a\varepsilon]-2(b-a)\gamma^+\gamma^-}, \quad (1)$$

$$\kappa(\omega) = \frac{[(b-a)\mu(\omega)+a](\gamma^+-\gamma^-)}{\mu_0\varepsilon_0\omega^2(1-\varepsilon_d)a(b-a)}, \quad (2)$$

where  $\mu_0$  and  $\varepsilon_0$  denote the permeability and permittivity of free space,  $\omega$  is the wave angular frequency,  $b$  is the cell's conducting strip half-width,  $a$  is the test sample half-width,  $\varepsilon$  is the effective permittivity, and  $\gamma^+$  and  $\gamma^-$  are the propagation coefficients for the forward and backward directions of propagation, respectively. They are analytically related to the  $S$  parameters of the cell containing the dielectric and magnetic samples.<sup>6</sup> Observe that Eqs. (1) and (2) are valid as long as we consider a situation in which the quasitransverse electromagnetic approximation, to obtain  $\mu$  and  $\kappa$ , is valid. One should bear in mind that the quantitative accuracy of this approach is limited: e.g., for the sample corresponding to a volume fraction of  $\text{Fe}_2\text{O}_3$  equal to 0.55, we estimate the absolute uncertainties to 0.008 for  $\mu''$  and 0.0006 for  $\kappa''$  at 1 GHz, respectively, where the errors are statistical and systematic. All experiments were carried out at room temperature.

### B. Materials

Commercially available ZnO and  $\gamma\text{-Fe}_2\text{O}_3$  powders were used as basic components of the samples studied here and were supplied from Nanophase Technologies Corp., Burr Ridge, IL. Control over the average grain size and shape was achieved by scanning electron microscopy (SEM). X-ray diffraction (XRD) confirmed the single-phase nature of the basic powders, and both XRD and SEM (Ref. 16) revealed random grain orientation and an average particle size of 23 nm for  $\text{Fe}_2\text{O}_3$  and 49 nm for ZnO. The size of the particles is below skin depth up to optical frequencies. Epoxy resin (Scotchcast 265) at a volume fraction of 12% was used as organic binder. The details of the fabrication procedure of these composite materials have been described previously.<sup>16</sup> As a result of this procedure, plaquettes of 1.8 mm thickness and about 5 mm long on each side were used for electromagnetic spectroscopy experiments. Throughout the text,  $f$  denotes the volume fraction of  $\text{Fe}_2\text{O}_3$ . The dispersibility of ferrimagnetic particles within the ZnO host matrix particles is of importance since grain boundaries contribute in a crucial way to the electrical and magnetic properties of granular materials. Even if there is no definitive method for evaluating dispersibility—and ultimately control over—of nanoparticles, SEM experiments provide support for a homogeneous dispersion during the mixing process and the interpretation of the results here and elsewhere.<sup>16</sup>

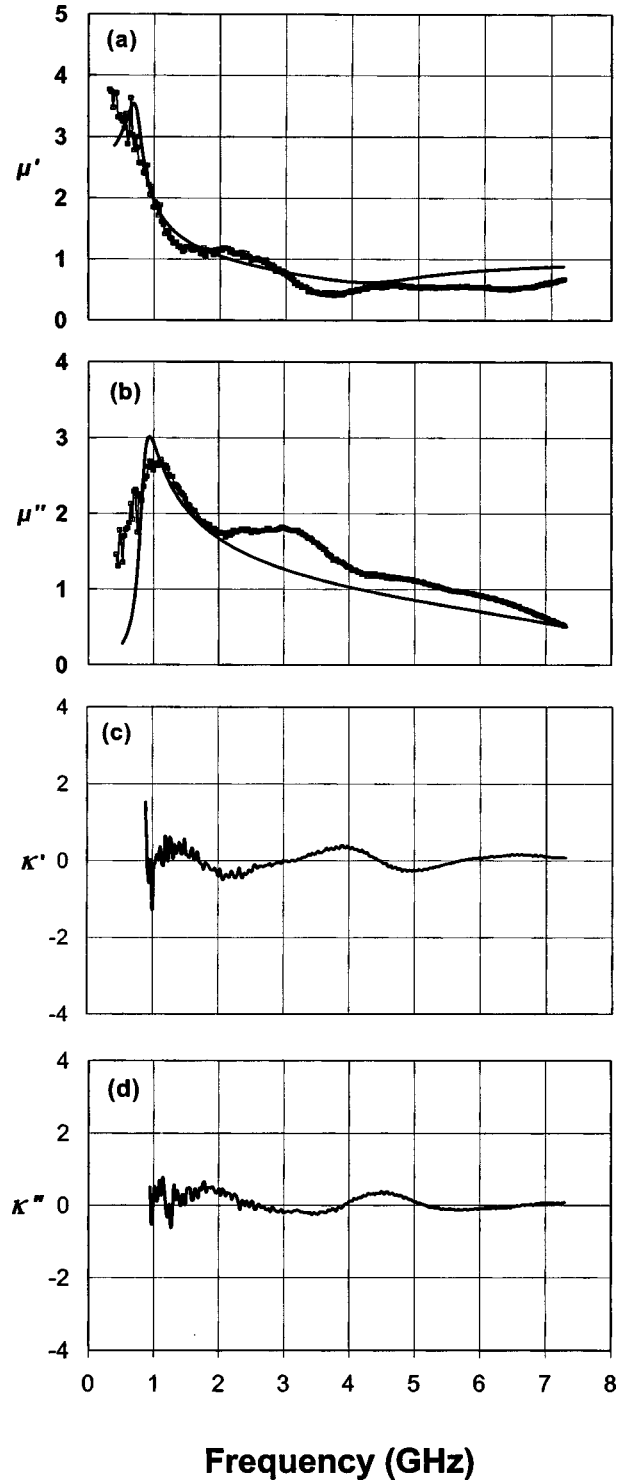


FIG. 2. The frequency dependence of the zero-field components  $\mu$  and  $\kappa$  of the permeability tensor for a ZnO/ $\text{Fe}_2\text{O}_3$  composite sample containing a volume fraction of  $\text{Fe}_2\text{O}_3$ ,  $f=0.55$ . (a) Real part  $\mu'$ , (b) imaginary part  $\mu''$ , (c) real part  $\kappa'$ , and (d) imaginary part  $\kappa''$ . Room temperature. The thin curve is a fit of the data to the SCMM model as described in the text.

### III. RESULTS

In Fig. 2 we present the real and imaginary parts of the permeability tensor components versus the frequency at zero

field for the sample containing a volume fraction of  $\text{Fe}_2\text{O}_3 = 0.55$ , corresponding to an internal porosity  $= 0.33$ . The first thing to note, in the zero-field spectra, is that the sample is macroscopically isotropic, i.e.,  $\kappa' \cong 0$  and  $\kappa'' \cong 0$ . These results are consistent with those observed in a previous work.<sup>16</sup> The gyromagnetic resonance at 1 GHz is accompanied by a second peak at 3 GHz. Such a peak is not instrumental and was ascribed to the polydispersity<sup>16</sup> of the nanophases since it follows the same composition and external magnetic field dependence as the main line. Figure 3 shows the same quantities measured in a field of 3 kOe and demonstrates the transport anisotropy found in this sample. A closer look at Fig. 3 reveals that the maximum of  $\mu''$  is coincident with the corresponding maximum of  $\kappa''$ . The position of the gyromagnetic peak is composition and field dependent. To obtain further insight into the magnetic properties of these materials, Fig. 4 summarizes the variation of the resonance frequency, determined either from the peak value of  $\mu''$  or  $\kappa''$ , as a function of the volume fraction of  $\text{Fe}_2\text{O}_3$ . Comparing the results for  $H=0$  and 3 kOe, one sees that in both cases the peak position shifts to lower frequency as the content of the magnetic phase is increased. Figure 5 shows the effect of varying the applied magnetic field on the resonance frequency, determined from  $\mu''$  and  $\kappa''$ , while keeping the volume fraction of  $\text{Fe}_2\text{O}_3$  constant ( $= 0.55$ ). The resonance frequency is shown in Fig. 5 to increase more than sixfold on going from  $H=0$  to 3 kOe. We interpret these results below in the context of a detailed investigation of the gyromagnetic resonance mode.

#### IV. DISCUSSION AND COMPARISON WITH THE MODEL

In this section, we will discuss the comparison between the experimental results and calculation based on a early work.<sup>14</sup> As far as we are concerned with very-long-wavelength physics—i.e., when the wavelength is much larger than the relevant length scale of inhomogeneities  $\xi$  (particle size, interparticles distance)—it is a good approximation to consider the effective medium assumption (EMA) made for describing the propagation of a well-defined coherent monochromatic electromagnetic properties in a random medium.<sup>4,14,19–22</sup> The predictive power of the EMA has in the past been known to be an appropriate means of estimating the permeability of heterostructures in which one of the components forms separate inclusions distributed randomly but uniformly in a matrix formed by the others. As one of us has shown in a previous work,<sup>14</sup> the magnetization dynamics problem in a composite structure of magnetic media could be understood by a self-consistent multiscale method (SCMM), in which microscopic information is combined with continuum description to obtain the required coarse graining. In a nutshell, this was done by deriving analytically the effective complex permeability from an effective theory consisting of the following ingredients: (1) the equivalent material is represented by a uniformly dispersed assembly of ellipsoidal inclusions randomly oriented in a dielectric host matrix, (2) each inclusion is assumed to have uniaxial anisotropy and is characterized by the orientation of its magnetization vector (easy axis) with respect to the external dc magnetic field  $H$ ,

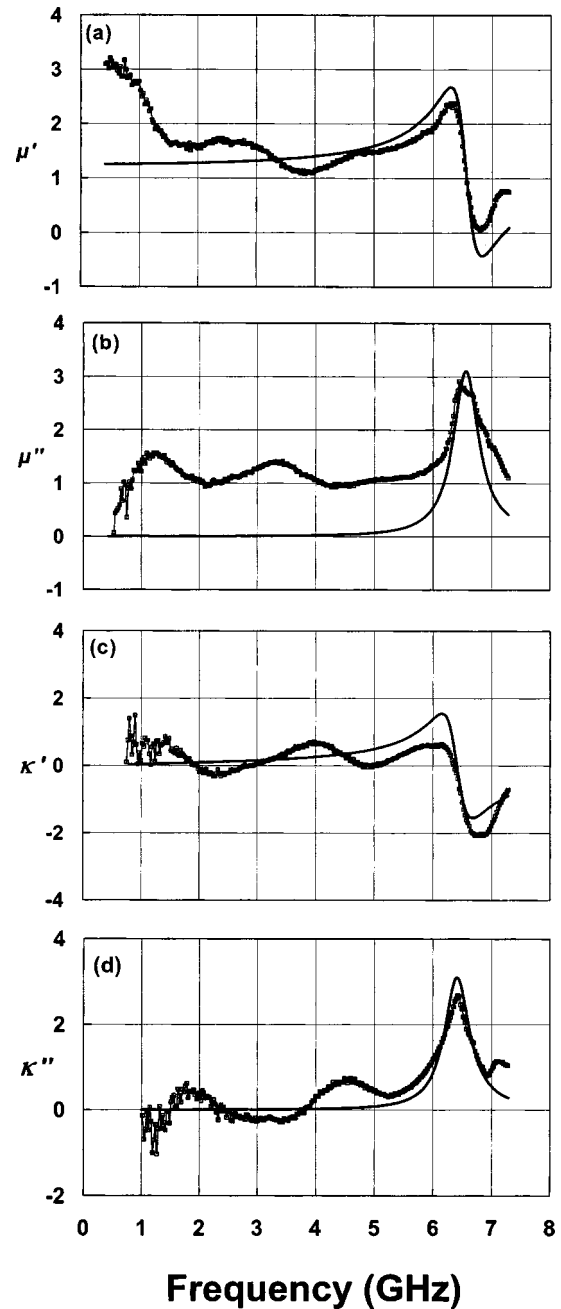


FIG. 3. The frequency dependence of the diagonal term  $\mu$  and nondiagonal term  $\kappa$  of the permeability tensor for a  $\text{ZnO}/\text{Fe}_2\text{O}_3$  composite sample containing a volume fraction of  $\text{Fe}_2\text{O}_3$ ,  $f = 0.55$ . The applied magnetic field is 3 kOe. (a) Real part  $\mu'$ , (b) imaginary part  $\mu''$ , (c) real part  $\kappa'$ , and (d) imaginary part  $\kappa''$ . Room temperature. The thin curve is a fit of the data to the SCMM model as described in the text.

(3) the permeability tensor of each inclusion is assumed to be of the Polder type with an effective anisotropy field  $H_{\text{eff}}$  which is deduced from  $H$  and the anisotropy field  $H_a$  via an internal energy minimization principle, and (4) then the EMA is used to determine the effective permeability tensor  $\vec{\mu}$  of the heterogeneous material. In addition, demagnetizing effects are taken into account by considering a demagnetizing tensor related to the shape anisotropy of the particles. In

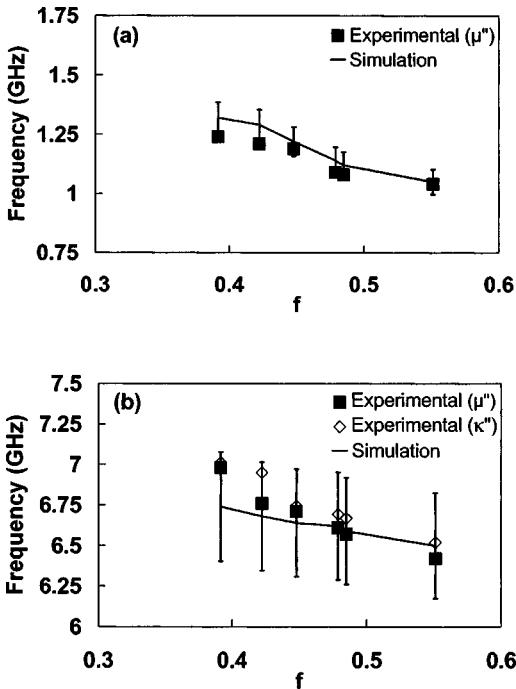


FIG. 4. The resonance frequency as a function of the volume fraction of  $\text{Fe}_2\text{O}_3$ . (a) Solid squares indicate data from  $\mu''$  and  $H=0$ . (b) Solid squares (open diamonds) indicate data from  $\mu''$  ( $\kappa''$ ) and  $H=3$  kOe. The solid line indicates the values predicted by the SCMM model.

all results presented here, the only adjustable parameter is the Gilbert damping parameter  $\alpha$  describing the dynamic behavior of the magnetization. For more detail on the method, see the previous work.<sup>14</sup> The expression for the permeability tensor was obtained under the assumption that the effect of interparticle interactions are included as a mean-field approximation. Both these assumptions are valid for the nanophases we are investigating here in the entire range of frequency explored.

With the SCMM thus parametrized to fit electromagnetic data, we have performed simulations of the frequency dependence of  $\mu(\omega)$  and  $\kappa(\omega)$ —i.e., thin curves in Figs. 2 and 3. Interestingly, the fit curves follow the frequency dependence of our data fairly well and all of the qualitative features of

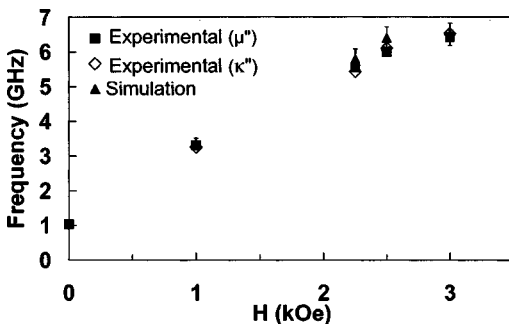


FIG. 5. The resonance frequency as a function of the applied magnetic field. The volume fraction of  $\text{Fe}_2\text{O}_3$  is  $=0.55$ . The data are obtained from  $\mu''$  (solid squares) and  $\kappa''$  (open diamonds). The solid triangles indicate the values predicted by the SCMM model.

the gyromagnetic resonance are reproduced. The fit gives a value of the Gilbert damping parameter  $\alpha=0.125\pm 0.01$ , which is consistent with recent theoretical models of the damping mechanism of ferrimagnetic particles.<sup>23,24</sup> As can be seen in Fig. 4, we achieve good quantitative agreement between the composition dependence of the resonance frequency and our data, although the error bars of the experimental data are too large for a precise comparison. These observations are also consistent with the field dependence, in the range of applied magnetic field explored, of the resonance mode predicted by the SCMM as shown in Fig. 5.

This result shows that the SCMM provides a reasonable description of the diagonal and nondiagonal terms of the permeability tensor. Let us examine a number of possible sources of the observed discrepancies. One possible concern with the present approach is that the standard effective (continuous) medium approximation underlying the present calculations was done under the simplifying assumption of spherical particles, even if there is a significant departure from perfect sphericity for the ZnO particles. However, the use of demagnetizing factors to account for the shape anisotropy of the ZnO particles leads to a small deviation between the mean-field theory and experiment. It should be borne in mind also that the model used here has randomly positioned grains, and as a result, even at low volume fractions of  $\text{Fe}_2\text{O}_3$  there exists the possibility of statistical clustering, which gives rise to some degree of exchange coupling between the magnetic particles. It was reported previously that the magnetic properties of  $\gamma\text{-Fe}_2\text{O}_3$  nanoparticles cannot be entirely described by a single-domain picture where all spins point in the same direction. This was attributed to surface effects.<sup>23</sup> In addition, the SCMM does not include information about the surface of the nanograins and clusters. Another possible source of discrepancy is the assumption of isotropic phenomenological damping which is taken to solve the dynamic equations for the anisotropic magnetic system considered here.

## V. CONCLUSIONS

In summary, the results presented here are the first direct measurements of the microwave permeability tensor of granular nanostructures under a static magnetic field excitation. From our findings, two key results emerge. First, we were able to probe the nondiagonal terms of the permeability tensor, i.e.,  $\kappa'-j\kappa''$ , which is a prominent feature of the magnetic-field-induced anisotropy in our granular heterostructures, as a function of frequency and composition. We observed how the resonance mode is altered by the content of the magnetic phase in these heterostructures and by the applied magnetic field. Second, the comparison of experimental observations with present calculations is supportive evidence that the SCMM has merit in order to characterize the mechanisms of the field-induced anisotropy of nanophases although a comprehensive micromagnetic description of the entire process, documenting the precise role of the different length scales, is not available. An important question raised by our data is how characteristic length scales describing the electromagnetism of nanostructures

may emerge from a multiscale model and how these length scales would vary with the type of granular heterostructures, the nature of the intergranular exchange and magnetostatic interactions, and the magnetic field.<sup>25</sup> The results of this paper also provide experimental input to help guide any future refinements of theories of the magnetic anisotropy in ultrafine magnetic particle systems that is capable of providing a consistent description that ultimately leads to a full understanding of its gyromagnetic behavior—e.g., the tensor structure of the phenomenological damping instead of one (isotropic) damping parameter.<sup>26</sup> Finally, these magnetic anisotropy effects may have profound practical applications

in advanced magnetoelectronic microwave devices<sup>27</sup> and in characterizing transport characteristics in artificial three-dimensional periodic materials with negative effective permittivities and permeabilities—i.e., left-handed media.<sup>28,29</sup>

#### ACKNOWLEDGMENTS

We wish to thank the M.E.N.S.R. for financial support to S.M. Technical assistance from D. Rozuel is gratefully appreciated. The Laboratoire d'Electronique et Systèmes de Télécommunications is Unité Mixte de Recherche C.N.R.S. 6165.

\*Also affiliated with Département de Physique, Université de Bretagne Occidentale. Corresponding author. FAX: 33-2 98 01 61 31. Electronic address: brosseau@univ-brest.fr

<sup>1</sup>For a review, see *Nanophase Materials: Synthesis, Properties, Applications*, edited by G. C. Hadjipanayis and R. W. Siegel (Kluwer Academic, New York, 1994).

<sup>2</sup>*Granular Nanoelectronics*, edited by D. Ferry, J. R. Barker, and C. Jacoboni, Vol. 251 of *NATO Advanced Study Institute, Series B: Physics* (Plenum, New York, 1990).

<sup>3</sup>R. C. O'Handley, *Modern Magnetic Materials* (Wiley, New York, 2000).

<sup>4</sup>C. Brosseau and A. Beroual, *Prog. Mater. Sci.* **48**, 373 (2003).

<sup>5</sup>J. Sykulski, J. Stoll, R. Sikora, K. Pawluk, J. Turowski, and Z. Zakrewski, *Computational Magnetism* (Chapman & Hall, London, 1995).

<sup>6</sup>P. Queffelec, S. Mallegol, and M. Le Floc'h, *IEEE Trans. Microwave Theory Tech.* **50**, 2128 (2002).

<sup>7</sup>M. Igarashi and Y. Naito, *IEEE Trans. Magn.* **13**, 1664 (1977).

<sup>8</sup>D. Polder, *Philos. Mag.* **40**, 99 (1949). See also D. Polder and J. Smit, *Rev. Mod. Phys.* **25**, 89 (1953).

<sup>9</sup>G. T. Rado, *Rev. Mod. Phys.* **25**, 81 (1953); *Phys. Rev.* **89**, 529 (1953).

<sup>10</sup>E. F. Schlömann, *J. Appl. Phys.* **41**, 204 (1970); *J. Phys. (Paris), Colloq.* **31**, 443 (1971).

<sup>11</sup>P. Gelin and K. Berthou-Pichavant, *IEEE Trans. Microwave Theory Tech.* **45**, 1185 (1997).

<sup>12</sup>J. P. Bouchaud and P. G. Zérah, *Phys. Rev. Lett.* **63**, 1000 (1989).

<sup>13</sup>A. Hubert and R. Schafer, *Magnetic Domains, The Analysis of Magnetic Microstructures* (Springer, Berlin, 1998).

<sup>14</sup>D. Bariou, P. Queffelec, P. Gelin, and M. Le Floc'h, *IEEE Trans. Magn.* **37**, 3885 (2001).

<sup>15</sup>Metal oxides have been widely used in catalysis, electrochemistry, optical fibers, and sensors and are of great technological importance: i.e., V. E. Henrich and P. A. Cox, *The Surface Science of Metal Oxides* (Cambridge University Press, Cambridge, England, 1994). C. E. Patton, in *Magnetic Oxides*, edited by D. J. Craik (Wiley, London, 1975).

<sup>16</sup>P. Talbot, A. M. Konn, and C. Brosseau, *J. Magn. Magn. Mater.* **249**, 483 (2002). This initial work has since been to encompass a more complete magnetic characterization of multicomponent metal oxides heterostructures and the reader is referred to C. Brosseau, J. Ben-Youssef, P. Talbot, and A.-M. Konn, *J. Appl. Phys.* **93**, 9243 (2003).

<sup>17</sup>R. E. Collin, *Field Theory of Guided Waves* (IEEE Press, New York, 1991).

<sup>18</sup>M. E. Hines, *IEEE Trans. Microwave Theory Tech.* **19**, 442 (1971).

<sup>19</sup>H. Suhl, *IEEE Trans. Magn.* **34**, 1834 (1998).

<sup>20</sup>D. Stroud, *Phys. Rev. B* **12**, 3368 (1975). See also D. J. Bergman and D. Stroud, in *Solid State Physics, Advances in Research and Applications*, edited by H. Ehrenreich and D. Turnbull (Academic, San Diego, 1992), Vol. 46, p. 147.

<sup>21</sup>R. Landauer, in *Electrical Transport and Optical Properties of Inhomogeneous Media*, edited by J. C. Garland and D. B. Tanner, *AIP Conf. Proc. No. 40* (AIP, New York, 1978), p. 2. See also R. Landauer, *J. Appl. Phys.* **23**, 779 (1952).

<sup>22</sup>A. Aharoni, *Introduction to the Theory of Ferromagnetism* (Clarendon, Oxford, 1996).

<sup>23</sup>H. Kachkachi, A. Ezzir, M. Nogues, and E. Tronc, *Eur. Phys. J. B* **14**, 681 (2000).

<sup>24</sup>P. Toneguzzo, G. Viau, O. Acher, F. Guillet, E. Bruneton, F. Fievet-Vincent, and F. Fievet, *J. Mater. Sci.* **35**, 3767 (2000). See also P. Toneguzzo, O. Acher, G. Viau, F. Guillet, E. Bruneton, F. Fievet-Vincent, and F. Fievet, *J. Appl. Phys.* **81**, 5546 (1997).

<sup>25</sup>W. F. Brown, *Micromagnetics* (Wiley, New York, 1963). See also W. F. Brown, *Phys. Rev.* **130**, 1677 (1963).

<sup>26</sup>V. L. Safonov, *J. Appl. Phys.* **91**, 8653 (2002). See also V. L. Safonov and H. N. Bertram, *Phys. Rev. B* **61**, R14 893 (2000).

<sup>27</sup>J. Helsing, *Principles of Microwave Ferrite Engineering* (Wiley, New York, 1969).

<sup>28</sup>D. R. Smith, W. J. Padilla, D. C. Vier, S. C. Nemat-Nasser, and S. Schultz, *Phys. Rev. Lett.* **84**, 4184 (2000).

<sup>29</sup>S. T. Chui and L. Hu, *Phys. Rev. B* **65**, 014407 (2002), and references therein.